Desalination and Water Treatment
www.deswater.com

doi: 10.1080/19443994.2015.1040846

57 (2016) 10572–10584
May

Taylor & Francis
Taylor & Francis Group

Cellulose acetate/poly(vinyl alcohol) and cellulose acetate/crosslinked poly (vinyl alcohol) blend membranes: preparation, characterization, and antifouling properties

Jun Yin, Haijuan Fan, Jiancheng Zhou*

School of Chemistry and Chemical Engineering, Southeast University, Jiangning District, Nanjing 211189, P.R. China, Tel. +86 13813016795; email: yinminghan@163.com (J. Yin), Tel. +86186 541 05986; email: hufan87@163.com (H. Fan), Tel./Fax: +86 025 52090620; email: jczhou@seu.edu.cn (J. Zhou)

Received 10 December 2013; Accepted 29 March 2015

ABSTRACT

Cellulose acetate (CA)/poly(vinyl alcohol) (PVA) blend membranes have been first prepared by non-solvent induced phase separation process. The pure water flux (PWF), hydrophilicity, and porosity increased with an increment in CA/PVA compositions up to 90/10. Then, polyvinyl pyrrolidone (PVP) as additive was added into the CA/PVA (90/10) casting solution. It was found that the PWF and porosity of CA/PVA/PVP blend membranes increased initially and then declined with the addition of PVP. Meanwhile, the effect of PVP content in CA/PVA blend membranes on fouling-resistant ability was studied using oil-in-water emulsion. The result indicated that all CA/PVA/PVP blend membranes had better antifouling property than CA/PVA membrane. If the PVA content in the casting solution increased to 20 wt%, the fabricating of membrane was difficult because of the strong hydrophilicity and large swelling capacity of PVA. Therefore, PVA was first crosslinked with glutaraldehyde (GA) as the crosslinking agent, followed by *in situ* blended with CA and PVP to fabricating the CA/crosslinked PVA (CPVA) (80/20)/PVP blend membrane. The effect of GA and PVP content on hydrophilicity, morphology, and performance of CA/CPVA (80/20)/PVP blend membranes were also discussed in detail.

Keywords: Cellulose acetate/poly(vinyl alcohol) blend membrane; Cellulose acetate/crosslinked poly(vinyl alcohol) blend membrane; Hydrophilicity; Oil-in-water emulsion; Anti-fouling property

1. Introduction

Nowadays, a large amount of oily wastewater is discharged by many industrial processes, such as food processing, metallurgical, petrochemical industries, and petroleum refineries. It was reported that more than two billion tons of wastewater is produced by oil refineries only in the Middle East and European Union countries [1,2]. The direct discharge of oily wastewater into the natural environment creates a major ecological problem throughout the world [3]. Therefore, it is necessary to purify the wastewater so that it can be reused to save water resources and to protect the environment.

Conventional treatment methods for oily wastewater mainly include gravity separation and skimming,

---

*Corresponding author.

1944-3994/1944-3986

dissolved air flotation (DAF), de-emulsification, biological treatment, sedimentation in a centrifugal field and in hydrocyclones [4–7]. Gravity separation is a commonly used method for primary treatment of oily wastewater, which has been proved to be effective in removing free oil when combined with skimming. DAF involves using air to increase the buoyancy of smaller oil droplets and improve their separation. Emulsified oil in the influent from gravity separation and skimming or DAF units can be removed by de-emulsification or thermal treatment. During de-emulsification, the oily wastewater is treated chemically to destabilize the oil-in-water emulsion and this treatment can be followed by gravity separation. The thermal treatment, which includes evaporation and incineration, is suitable for managing many types of oily water. But it involves high energy costs, and the condensate has to be treated to remove oils in the vapors. Generally, conventional treatment methods have been proved to be effective in treating oily wastewater especially when they are combined together. However, there are numerous disadvantages such as low operation efficiency, high cost, and recontamination problems [8]. In addition, these methods are not effective for stable oil-in-water emulsions separation, where oil droplets are steadily dispersed in water under the help of surfactants. As a result of this, new treatment methods for oily wastewater have to be established in order to overcome these disadvantages.

There is a growing tendency to employ several kinds of membrane separation technologies for treating oily wastewater, which has been generally accepted as an excellent method with lower cost, higher operation efficiency, and less pollution [9–11]. Because of its suitable pore sizes and the capability of removing emulsified oil droplets without any de-emulsification processes, ultrafiltration has been demonstrated as an efficient method and a pretreatment step before nanofiltration and reverse osmosis in oil-in-water emulsion separation [12–14]. However, one challenge, which limits their wide application in the oil-in-water emulsion separation, comes from the severe membrane fouling caused by the adsorption and deposition of oil droplets on the membrane surface that can block the membrane pores, resulting in a significant decline of permeate flux [15]. It is commonly accepted that increasing the membrane surface hydrophilicity can dramatically mitigate membrane fouling. Therefore, hydrophilic membranes, such as cellulose acetate (CA) membrane, have become the preferential choice to application in oil-in-water emulsion separation. As an environmental-friendly product [16], CA becomes an interesting candidate polymer with regard to its low price, moderate chlorine resistance, good biocompatibility, and high hydrophilicity [17]. However, in many cases, the highly hydrophilic property of CA slows the diffusion of the non-solvent (water) and retards coagulation during the phase inversion process, resulting in a dense skin layer and a low permeate flux [18–20]. Consequently, the modification of CA membrane is necessary. Since the blending of appropriate polymer with CA, it is a versatile technique for the modification of CA membrane. CA has been blended with several high-performance polymers such as Pluronic F127 [20], polyethersulfone [21], polyurethane [19,22], poly (etheretherketone) [23], sulfonated polysulfone [24] in order to improve the properties of CA membrane. Recently, poly(vinyl alcohol) (PVA) have attracted increasing interest as a promising membrane material due to its highly hydrophilic, non toxic, and biocompatible polymer with excellent film-forming properties, high mechanical strength, low fouling potential, and long-term temperature and strong pH stability [25]. Therefore, it is expected that bringing together PVA and CA would conserve their superior properties in the final mixture and concurrently reduce their poor characteristics.

In this study, CA was considered as the main polymer for membrane backbone. PVA was added to the casting solution in the presence of polyvinyl pyrrolidone (PVP) as additive. The effects of PVA content and PVP content on hydrophilicity, morphology, and the oil-in-water emulsion separation performance of blend membranes were investigated. However, the strong hydrophilicity and large swelling capacity of PVA made the fabrication of CA/PVA (80/20) blend membrane difficult. The high swelling capacity of PVA can be overcome by crosslinking reactions with the consumption of some of the OH groups, as the OH groups are responsible for the hydrophilicity [26]. Therefore, PVA was first crosslinked with glutaraldehyde (GA) as the crosslinking agent, followed by *in situ* blended with CA and PVP to fabricating the CA/crosslinked PVA (CPVA) (80/20)/PVP blend membrane by classical phase inversion method. The effect of GA and PVP content on hydrophilicity, morphology, and performance of CA/CPVA (80/20)/PVP blend membranes were also investigated in detail.

2. Experimental

2.1. Materials

CA (CA, acetyl content 40%), PVA (PVA, with a degree of polymerization of 1,750 ± 50), PVP (PVP, with $M_w = 58{,}000$ g/mol), dimethyl sulfoxide (DMSO), sulfuric acid (98 wt%), GA (GA, 25 wt%), sodium dodecyl sulfate (SDS) were purchased from Aladdin Reagent Company of analytical grade and used as received. Engine oil (20W-40) was purchased from Exxon Mobil Oil Company. Deionized water purified from Millipore system was used to prepare all solutions as needed in the study.

2.2. Preparation of CA/PVA/PVP blend membranes

All the membranes were prepared by classical phase inversion method. Table 1 shows the composition of CA/PVA/PVP casting solutions. For all casting solutions, the total polymer content to total casting solution was 12 wt%, keeping the solvent and PVP concentration at 88 wt%. The casting solution obtained was left still for about 12 h to allow complete release of bubbles. After that, it was cast onto a glass plate using a stainless-steel knife to get a casting film of 250 μm thickness, exposed to the atmosphere for 15 s, and then immersed into a coagulation bath of deionized water. After peeling off from the glass plate, the prepared membranes were kept in deionized water for more than 12 h to remove residual solvent before test.

2.3. Preparation of CA/CPVA/PVP blend membranes

1.2 g PVA was added and dissolved into DMSO (keeping the DMSO and PVP concentration at 88 wt%) with constant stirring for 4 h. After PVA was completely dissolved, a dope of concentrated sulfuric acid and GA solution (0.2, 0.4, 0.6, and 0.8 wt% based on the weight of PVA) were added into the above solution and fully dissolved after stirring at 55℃ for about 4 h, followed by adding 4.8 g CA (keeping the CA and PVA concentration at 12 wt%) and different contents PVP into the casting solution and mechanically stirring at 60℃ for at least 12 h. The casting solution obtained was left still for about 12 h to allow complete release of bubbles. After that, it was cast onto a glass plate using a stainless-steel knife to get a casting film of 250 μm thickness, exposed to the atmosphere for 15 s, and then immersed into a coagulation bath of deionized water. After peeling off from the glass plate, the prepared membranes were kept in deionized water for more than 12 h to remove residual solvent before test. Compositions of the casting solutions are presented in Table 2.

2.4. Solution viscosity measurements

The viscosities of the prepared casting solutions were measured with a NDJ-8S digital viscometer at a constant temperature of 25℃.

2.5. Membrane structure characterization

FT-IR spectra of CA/PVA and CA/CPVA blend membranes were obtained for spectroscopic investigation. All FT-IR spectra were recorded by the attenuated total reflection (ATR) technique using Nicolet 5700 FT-IR spectrometer with horizontal ATR device (Ge, 45°). Thirty-two scans were taken with 4 cm^{-1} resolution between 4,000 and 500 cm^{-1}.

The cross-sectional morphologies of membranes were characterized by SEM (JSM-6360LV). Before SEM analysis, the membrane samples were dehydrated through graded ethanol series and then dried at room temperature [27]. Subsequently, they were snapped in liquid nitrogen and sputter-coated with gold to make them conductive.

Table 1
The compositions of CA/PVA/PVP casting solutions

Composition (wt%)		Additive (wt%)	
CA	PVA	PVP	DMSO (wt%)
100	0	0	88
90	10	0	88
80	20	0	88
90	10	1	87
90	10	3	85
90	10	5	83
90	10	7	81

Note: Total CA and PVA concentration = 12 wt%, the fabrication of CA/PVA (80/20) blend membrane was difficult.

Table 2
The compositions of casting solutions of CA/CPVA blend membranes

Composition (wt%)		Crosslink reagent	Additive	
CA	PVA	GA (wt%)	PVP (wt%)	DMSO (wt%)
80	20	0.2	0	88
80	20	0.4	0	88
80	20	0.6	0	88
80	20	0.8	0	88
80	20	0.4	1	87
80	20	0.4	3	85
80	20	0.4	5	83
80	20	0.4	7	81

Note: Total CA and PVA concentration = 12 wt%, the content of GA based on the weight of PVA.

The membrane porosity was determined by the mass loss of wet membrane after drying. The membrane sample being wetted thoroughly was mopped with water on the surface and weighed under wet status. Then, the membrane sample was dried until a constant mass was obtained. Porosity, ε, i.e. the ratio of pore volume to geometrical volume, for the membranes was obtained by using following equation:

$$\varepsilon = \frac{(m_\mathrm{w} - m_\mathrm{d})}{AL_\rho} \tag{1}$$

where m_w (g) is the wet membrane weight, m_d (g) is the dry membrane weight, and A, L, ρ are the wet membrane effective area (cm^2), the wet membrane thickness (cm), and the pure water density (g/cm^3), respectively. In order to minimize experimental error, all measurements were repeated three times and the average values were obtained.

In order to examine variations in the surface wetting characteristics of the CA/PVA/PVP and CA/CPVA/PVP blend membranes, water contact angle was measured for membrane surface using a contact angle measuring instrument (JC-2000C1). Deionized water was used as the probe liquid in all measurements. To minimize the experimental error, the contact angles were measured at three random locations for each sample and the average number was reported.

2.6. *Oil-in-water emulsion preparation*

The oil-in-water emulsion was prepared as follows: 0.45 g Engine oil (20W-40) and 0.05 g SDS were added to 500 mL deionized water, and then mixed by high-shear emulsifying dispersion for 30 min to obtain oil-in-water emulsion. The emulsion was stored at room temperature and used in 24 h.

2.7. *Membrane performance characterization*

A dead-end stirred cell (CB-380, the membrane area is 45.3 cm^2) filtration system connected with solution buffer reservoir and nitrogen gas cylinder was conducted to evaluate membrane permeability, retention, and antifouling properties. The ultrafiltration experiment was carried out at 25 ± 1℃ with a near-surface stirring speed of 300 rpm. The model feed solution was oil-in-water emulsion (0.9 g/L). The detailed operation process consisted of three steps: (1) each membrane was initially pressured at 0.15 MPa for 30 min, and then the operation pressure was set at 0.1 MPa during deionized water filtration process, the PWF was measured as J_W1; (2) then 0.9 g/L oil-in-water emulsion was permeated through the membrane under 0.1 MPa; (3) after 1 h oil-in-water emulsion ultrafiltration, the fouled membrane was washed with deionized water for about 30 min, and then the PWF of cleaned membrane was remeasured as J_W2. The steady PWF J_W1, J_W2 (L/m^2 h) were defined by following equation:

$$J = \frac{V}{At} \tag{2}$$

where V (L) was the volume of permeated water, A (m^2) was the membrane area, and t (h) was the operation time. The rejection ratios of oil were calculated by determining the concentration of oil in the feed and permeate solutions by UV-spectrophotometer (UV-9200) at a wavelength of 531 nm. The oil rejection ratio, r, was calculated by using following equation:

$$r = (1 - C_\mathrm{p} \ / \ C_\mathrm{f}) \times 100\% \tag{3}$$

where C_p and C_f were the oil concentration of permeate and feed solutions, respectively. In order to evaluate the oil-fouling-resistant ability of membranes, flux recovery ratio (FRR) was calculated using the following Eq. (4):

$$\mathrm{FRR} = \frac{J_\mathrm{w2}}{J_\mathrm{w1}} \times 100\% \tag{4}$$

3. Results and discussion

3.1. *Effect of CA/PVA composition*

ATR-FT-IR spectra of the pure CA membrane and the CA/PVA (90/10) blend membrane are shown in Fig. 1. As can be seen, the pure CA membrane shows a broad absorption band at 3,460 cm^{-1}, which is assigned to the stretching vibration of O–H. Moreover, the peak located at 1,740 cm^{-1} is assigned for the carbonyl stretching of CA and two strong peaks at around 1,230 and 1,050 cm^{-1} are associated with the asymmetric and symmetric stretching vibration of the C–O–C bond. By contrast, as for the blend membrane, the carbonyl peak intensity change is not prominent, while the O–H stretching vibration intensity increases, which can enhance the membrane's hydrophilicity.

The effect of CA/PVA blend ratio on membrane morphology is shown in Fig. 2. The membranes were prepared from 100/0, 90/10 blend ratio of CA/PVA with the constant concentration (12 wt%) of polymers and without addition of PVP in the casing solutions. Fig. 2 depicts the SEM cross-sectional photographs of

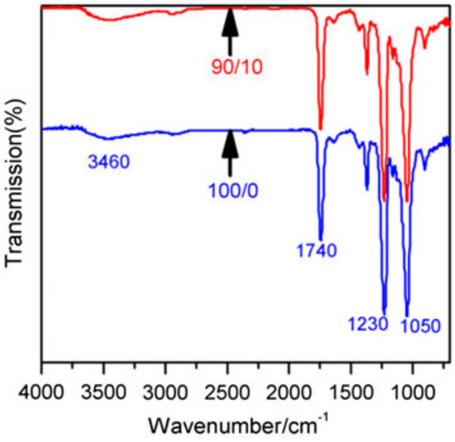

Fig. 1. ATR-FT-IR spectra of CA/PVA blend membranes with different ratio of CA and PVA.

the membranes. The membrane prepared from pure CA exhibits finger-like cavities and all small sponge-like pores developed in the sublayer. Comparing with this, the addition of 10 wt% PVA into the casting solution causes the formation of macrovoids. Furthermore, in this case, more porous structure beneath the skin layer of the membrane was observed (Fig. 2(b)), which in consequence improves the porosity and PWF of the membrane (as shown in Table 3). The changes in morphology can be attributed to the changes in the blend composition by the addition of PVA. We can expect an enhancement of the membrane surface hydrophilicity by blend with PVA (as shown in Table 3). In this study, the presence of PVA as a hydrophilic composition may intensify thermodynamic instability of the casting solution and this result in intensive increase of mutual diffusivities between the non-solvent (water) and the solvent (DMSO) in the system during solidification of the casting solution. This facilitates the formation of macrovoids in the membrane structure. If the PVA content in the casting solution increases to more than 10 wt%, the fabricating of membrane is difficult due to the strong hydrophilicity and large swelling capacity of PVA. Thus, the 90/10 blend ratio of CA/PVA has been chosen for further investigation.

3.2. *Effect of PVP content on CA/PVA blend membrane's morphology and hydrophilicity*

In order to further improve the performance of CA/PVA blend membrane, the influences of different content of PVP has been investigated. In our experiments, the 90/10 blend ratio of CA/PVA and total polymer concentration of 12 wt% are selected. Fig. 3 shows the cross-sectional morphologies of membranes prepared from CA/PVA (90/10) with 0, 1, 3, 5, and 7 wt% of PVP. As can be seen, all of the membranes exhibit typical asymmetrical structure of ultrafiltration membrane including a dense top layer (skin layer, air side), a porous sublayer (support layer), and a small portion of sponge-like pores near bottom surface (glass side). Clearly, the skin layer acts as a separation layer and the support layer provides the mechanical strength. The sublayer seems to have finger-like cavities beneath the top surface layer and macrovoids near the bottom. On the other hand, with increasing PVP content (Fig. 3(b)–(d)), the skin layer seems to be looser, and the finger-like pores become longer and better vertically interconnect with transfixion from membrane top layer to sublayer. The macrovoids

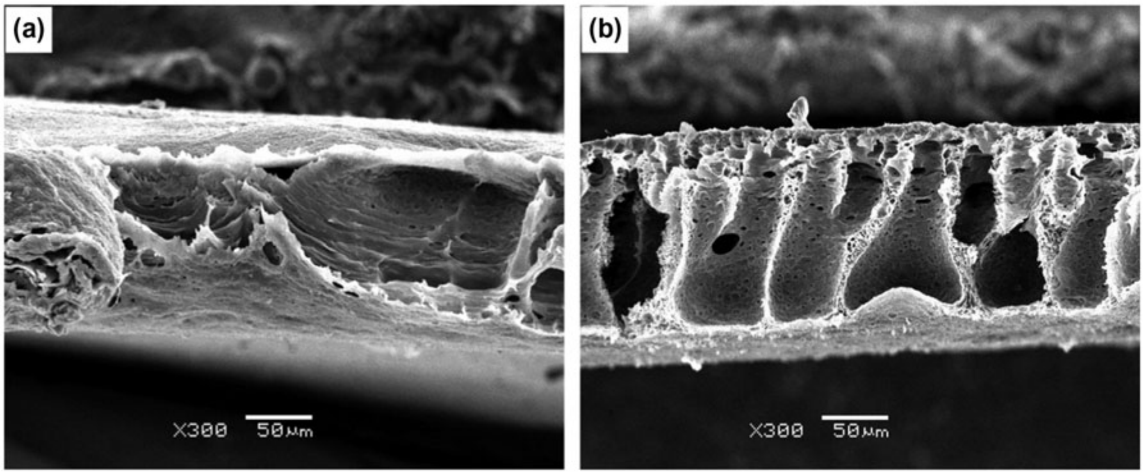

Fig. 2. Cross-sectional SEM images of (a) 100/0 and (b) 90/10 CA/PVA blend membranes.

Table 3
Effect of blend ratio of CA and PVA on the performance of blend membranes

Membrane	Porosity (%)	Contact angle (°)	PWF (L/m^2 h)
100/0	78.23 ± 0.47	68.5 ± 1.2	412.8 ± 12.4
90/10	80.66 ± 0.29	63.8 ± 0.4	482.9 ± 20.8

Note: Total polymer concentration = 12 wt%, additive concentration = 0 wt%. Data were means ± SD (n = 3).

beneath the finger-like cavities have fully developed and the pore walls among macrovoids become looser with some channel-like pores. With the continuous increasing of PVP content (Fig. 3(e)), the skin layer seems to be denser, the macrovoids decrease in number and become smaller, and the sponge-like pores near bottom surface increase.

The existence of PVP in the casting solutions has two effects. Presence of PVP, as a material with non-solvent properties, decreases the thermodynamic stability of the casting solution, and consequently causes instantaneous demixing in the coagulation bath, resulting in the formation of high porosity and facilitation of macrovoid formation in the membrane sublayer. With increasing PVP content, the increased viscosity of the casting solution (as shown in Table 4) slows the diffusional exchange rate of the solvent (DMSO) and non-solvent (water) during the solidification process and consequently hinders instantaneous demixing. This can lead to delayed demixing and, consequently, the suppression of macrovoids and formation of a dense structure.

The hydrophilicity of the membranes is evaluated by a water contact angle measurement, which is the most convenient way to assess the hydrophilicity and wetting characteristics of membrane surface. As shown in Table 4, the membrane cast from CA/PVA without PVP has the highest contact angle (63.8°). Comparatively, the increased content of PVP decreases the contact angles, suggesting enhanced hydrophilicity of the membrane surface. It should be noted that PVP is more hydrophilic in comparison with CA/PVA and consequently its presence in the membrane structure increases the membrane hydrophilicity. Also, molecular weight of PVP employed in this work is not low and consequently it cannot be completely washed out quickly with the solvent during formation of the membranes as well as cleaning of the membranes [28]. Thus, it can be expected that some of the PVP are entrapped in the pores and attach onto the membrane surface. Quantity of the residual PVP, which has a direct relationship with membrane hydrophilicity, highly depends on the content added into the casting solution. But further addition of 7 wt% PVP, the increased viscosity of the casting solution hinders the migration of PVP to the membrane surface, which reduces the membrane's hydrophilicity.

3.3. Separation and antifouling performances of CA/PVA blend membranes with different PVP content

After initial compaction of the membranes for 0.5 h at 150 kPa, the membranes were thoroughly washed with deionized water and subjected to a pressure of 100 kPa to measure the PWF. Fig. 4 clearly shows that the PWF is significantly affected by the content of PVP added into casting solution. It is clear that the CA/PVA membrane without PVP exhibits PWF of 482.9 L/m^2 h. Then, the value increases at first and reaches to a maximum when the content of PVP is 3 wt%. However, the opposite phenomenon is observed with the continuous addition of PVP in the CA/PVA casting solution. In general, the PWF is determined by the pore number, pore size, and hydrophilicity of the membrane [29]. As commented before, When 1 wt% PVP was added into the casting solution, there are relatively large pores in the surface (as shown in Fig. 4 oil rejection) compare to the pure CA/PVA membrane and enhanced hydrophilicity exhibits PWF of 488.9 L/m^2 h. As for the change tendency of PWF with the presence of PVP, the synergetic effect of decreased porosity and enhanced hydrophilicity should be considered. Since the hydrophilicity of CA/PVA/PVP (5 wt%) and CA/PVA/PVP (7 wt%) membranes are higher than that of CA/PVA/PVP (3 wt%) membrane, the increase of the membrane hydrophilicity is inevitable and it can reduce the interfacial resistance and promote water molecules to pass through the membrane. But, PWF don't agree with the hydrophilicity. The reason for this result is that the influence of the porosity is more significant.

To evaluate the antifouling properties of membranes, the FRRs of different membranes are calculated and represented in Table 4. It can be seen that the FRR of PVP blended membranes are high compared to the neat CA/PVA membrane. This indicates that the blend membranes have high recycling

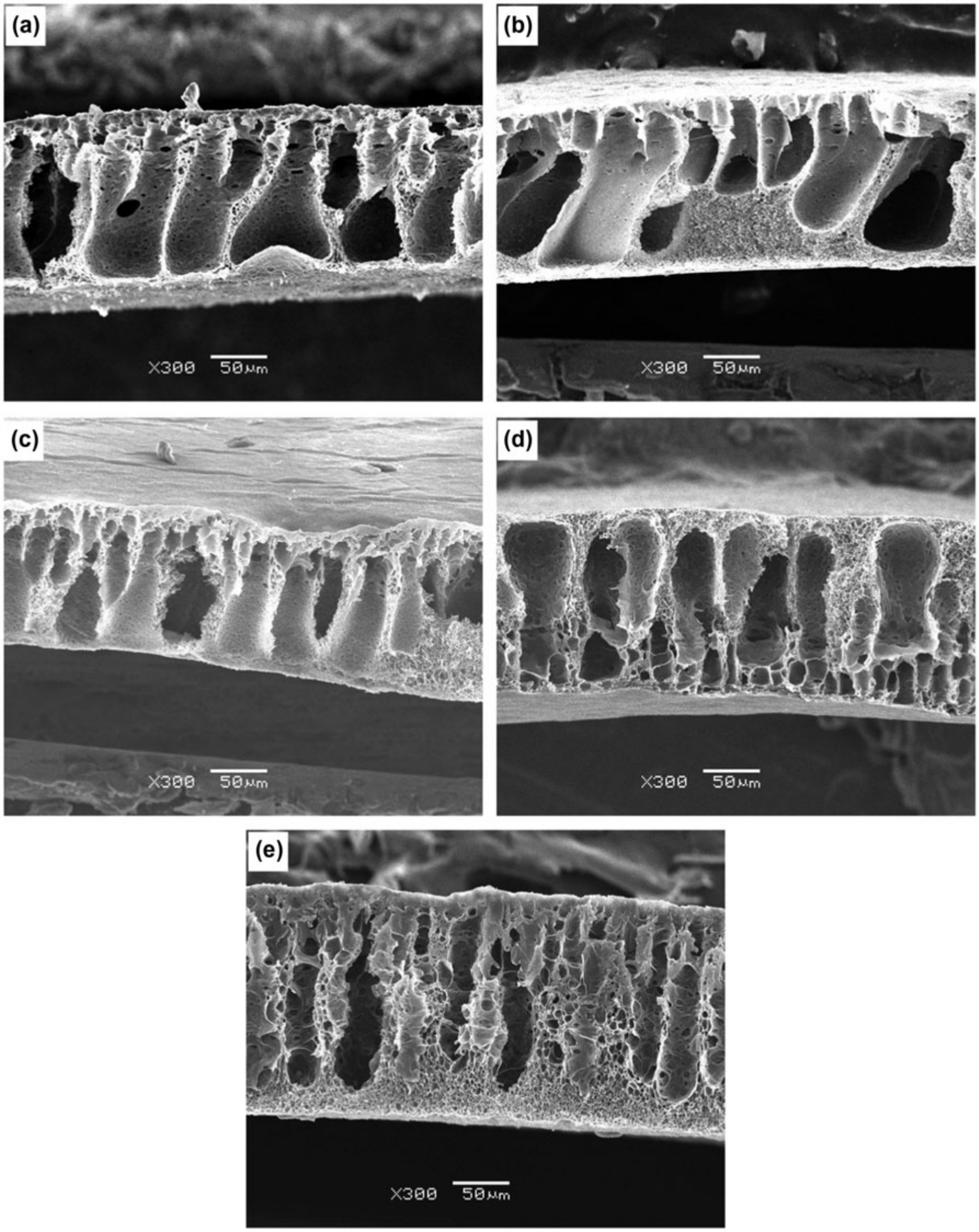

Fig. 3. Cross-sectional SEM images of CA/PVA blend membranes with different PVP content: (a) PVP 0 wt%, (b) PVP 1 wt%, (c) PVP 3 wt%, (d) PVP 5 wt%, and (e) PVP 7 wt%.

property. As revealed in Table 4, the surfaces of CA/PVA/PVP membranes are more hydrophilic compare to the CA/PVA membrane. It is well established that the membranes with more hydrophilicity have lower tendency to be fouled. Therefore, hydrophobic adsorption between oil and surface of CA/PVA/PVP blend membranes is diminished and deposited foulants are readily removed during membrane cleaning.

Table 4
Porosity, contact angle, FRR, and viscosity of CA/PVA membrane with different PVP content

Membrane	Porosity (%)	Contact angle (°)	FRR (%)	Viscosity (Pa s)
CA/PVA/PVP (0%)	80.66 ± 0.29	63.8 ± 0.4	70.6 ± 0.3	8.78 ± 0.76
CA/PVA/PVP (1%)	86.01 ± 1.71	59.0 ± 0.6	74.8 ± 0.7	10.24 ± 0.64
CA/PVA/PVP (3%)	82.22 ± 1.21	56.2 ± 0.8	83.5 ± 2.1	15.12 ± 1.31
CA/PVA/PVP (5%)	79.97 ± 0.41	52.5 ± 0.3	81.4 ± 1.3	17.86 ± 1.15
CA/PVA/PVP (7%)	75.58 ± 0.49	53.5 ± 0.4	80.8 ± 1.1	25.62 ± 1.32

Note: Total polymer concentration = 12 wt%, CA/PVA = 90/10. Data were means ± SD (n = 3).

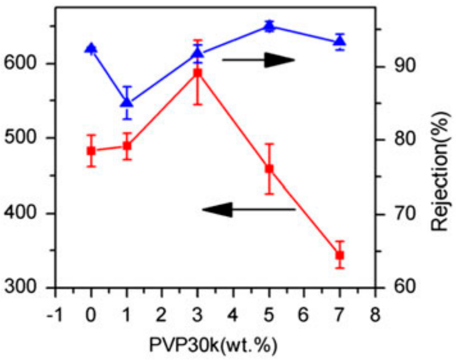

Fig. 4. PWF and oil rejection of CA/PVA blend membranes with different PVP content. Data were means ± SD (n = 3).

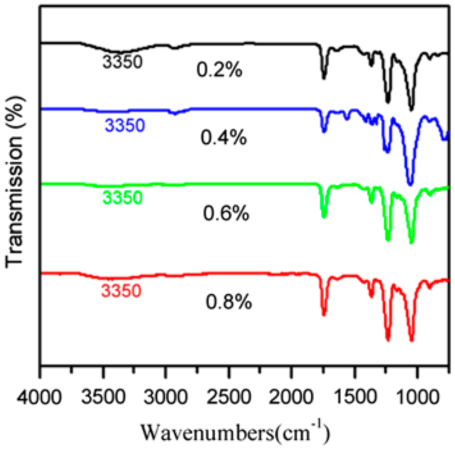

Fig. 5. ATR-FT-IR spectra of CA/CPVA blend membranes with 0.2 wt%, 0.4 wt%, 0.6 wt%, and 0.8 wt% GA, respectively.

3.4. The fabrication of CA/CPVA blend membranes

As analyzed before, the fabricating of CA/PVA (80/20) blend membrane is difficult because of the strong hydrophilicity and large swelling capacity of PVA. Therefore, PVA was first crosslinked with GA, followed by *in situ* blended with CA to fabricate the CA/CPVA (80/20) blend membrane by classical phase inversion method.

3.4.1. Effect of the crosslinking reagent GA content on the membrane hydrophilicity and morphology

As shown in Fig. 5, increasing the crosslinking reagent GA content from 0.2 to 0.6 wt% causes the hydroxyl groups of the PVA to react more with the aldehyde groups of GA, which would result in reduction of the intensity of O–H peak in wavenumber 3,350 cm^{-1}, but with further addition of 0.8 wt% GA into the casting solution. The peak intensity of O–H increases, indicating that there is possible formation of the acetal bridges among the pendant hydroxyl groups of PVA chains when GA was used with acid as a catalyst [30].

As shown in Fig. 6(c), the contact angles of the prepared membranes exhibit the decreasing hydrophilicity. Increasing the crosslinking reagent GA's content causes the hydroxyl groups of the PVA to react more with the aldehyde groups of GA, which cause the membrane to having less hydrophilicity behavior.

As presented in Fig. 7(a), the membrane exhibits an asymmetric structure consisting of a dense top layer and a porous sublayer (short finger-like pores and macrovoids). After the addition of 0.4 wt% GA into the casting solution, the as-prepared membrane has less dense top layer, the finger-like pores become longer and better vertically interconnected with transfixion from membrane top layer to sublayer. The macrovoids beneath the finger-like cavities have fully developed and the pore walls among macrovoids loose with some channel-like pores (Fig. 7(b)). But when the content of GA was increased to 0.6 wt%, the macrovoids decrease in number and become smaller and the sponge-like pores near bottom surface increases (Fig. 7(c)). When the content of GA in the casting solution is further increased to 0.8 wt%, the skin layer seems to be denser and the macrovoids

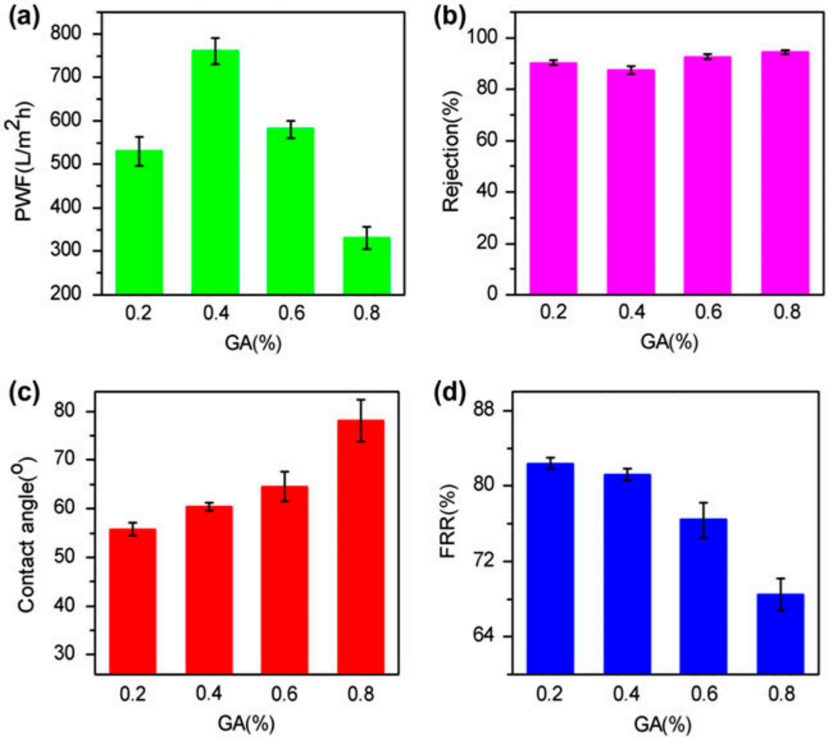

Fig. 6. (a) PWF, (b) oil rejection, (c) water contact angle, and (d) flux FRR of CA/CPVA blend membranes with 0.2 wt%, 0.4 wt%, 0.6 wt%, and 0.8 wt% GA, respectively. Data were means ± SD (*n* = 3).

almost disappear. The entire cross-section exhibits a dense structure (Fig. 7(d)).

3.4.2. *Effect of the crosslinking reagent GA content on the membrane separation and antifouling performances*

As listed in Fig. 6(a), the PWF increases and reaches to a maximum when the content of GA is 0.4 wt%. Nevertheless, it decreases with the continuous addition of GA. Generally, the PWF is determined by the pore number, pore size, hydrophilicity, and cross-sectional morphology of the membrane. When 0.4 wt% GA was added into the casting solution, there are relatively large pores on the surface (Fig. 6(b)), better vertically interconnect finger-like pores (Fig. 7(b)). Obviously, these factors should be responsible for the highest value of the PWF. However, with the continuous addition of GA (0.6 and 0.8 wt%), the surface pore size becomes smaller and lower porosity, less hydrophilic surface, and denser membrane structure are obtained. As a consequence, the decrease of the PWF is inevitable.

To evaluate the antifouling properties of membranes, the FRR of different membranes are calculated and represented in Fig. 6(d). It can be seen that the FRR of the membranes decrease consecutively with the increasing content of GA. This change tendency is consistent with the surface hydrophilicity. Thus, the CA/CPVA/GA (0.4 wt%) has been chosen for further investigation, which result from the as-prepared membrane exhibiting the highest PWF (760.2 L/m^2 h) and high FRR (81.2%).

3.4.3. *Effect of the PVP content on the CA/CPVA membrane separation and antifouling performances*

As discussed in Section 3.3, the separation and antifouling performances of the hybrid membranes were enhanced with the addition of PVP. In this section, we also used the PVP as additive to improve the performances of the CA/CPVA membrane. As shown in Fig. 8(a), the PWF of CA/CPVA/PVP blend membranes increased initially and then declined with the addition of PVP, the optimal PVP content was 3 wt%, with the highest PWF (928.7 L/m^2 h) and the highest FRR (86.3%). Compare Fig. 4 and Table 4 with Fig. 8, it can safely draw a conclusion that the CA/CPVA/PVP blend membrane exhibited higher PWF and stronger antifouling ability than the CA/PVA/PVP blend membrane.

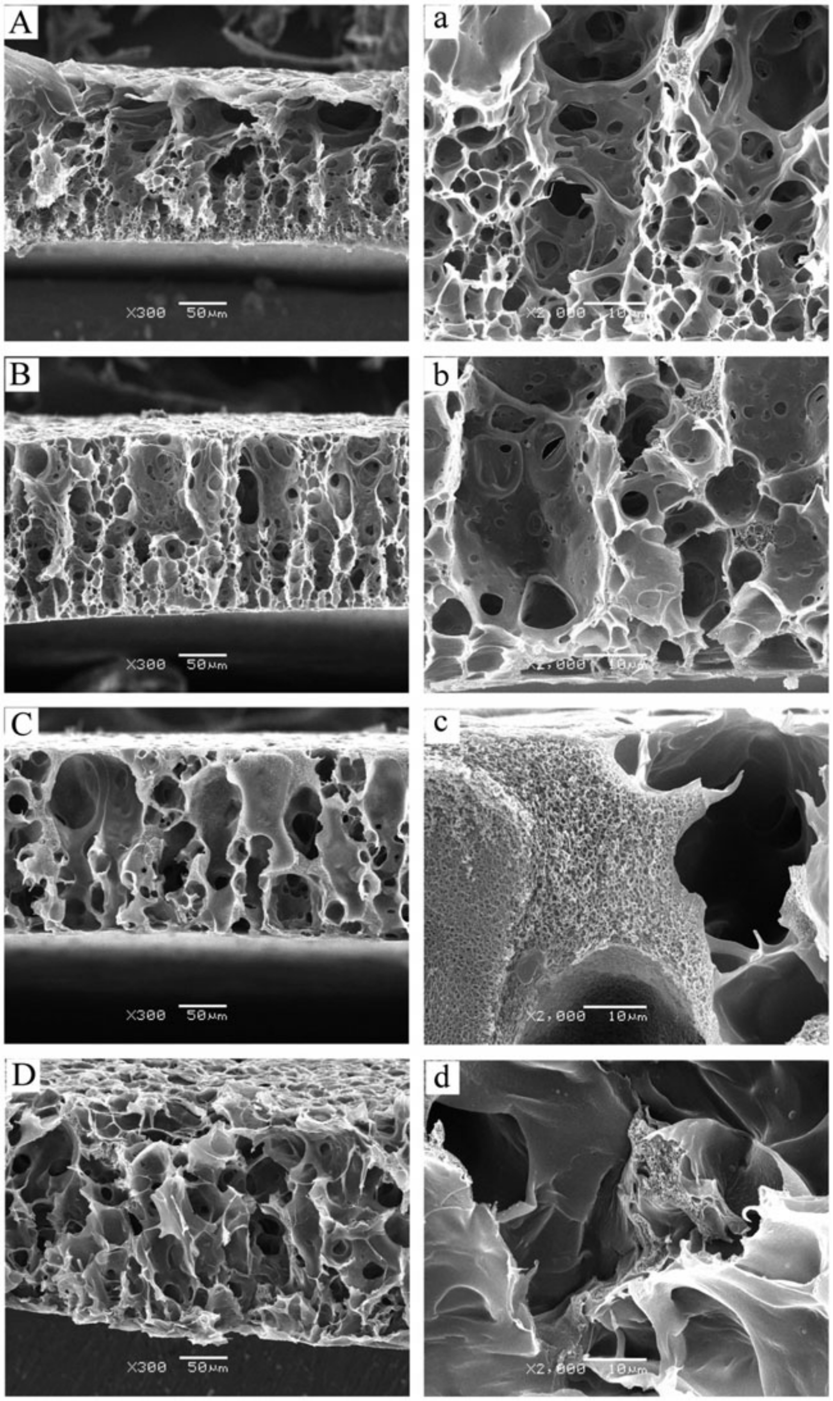

Fig. 7. Cross-sectional SEM images of CA/CPVA blend membranes with (A) 0.2 wt%, (B) 0.4 wt%, (C) 0.6 wt%, and (D) 0.8 wt% GA, respectively, and the amplified images of CA/CPVA blend membranes with (a) 0.2 wt%, (b) 0.4 wt%, (c) 0.6 wt%, and (d) 0.8 wt% GA, respectively.

3.4.4. Stability of CPVA in the CA/CPVA hybrid membrane

The stability of the membrane is crucial in the oily wastewater treatment, which can be investigated by measuring the water contact angle, oil rejection, and PWF of the membrane before and after shaking. In this work, the membranes of CA/PVA and CA/CPVA without the addition of PVP were chosen, which were

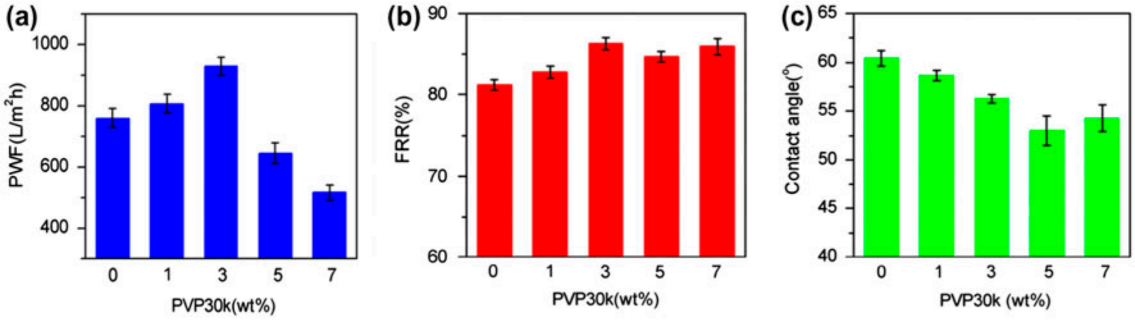

Fig. 8. (a) PWF, (b) FRR, and (c) water contact angle of CA/CPVA blend membranes with different PVP content. Data were means ± SD (n = 3).

immersed into deionized water under continuously shaking at 50℃ for different time span (3, 6, and 9 d). During the shaking process, the deionized water was replaced every day. Then, the washed membranes were dried and detected by water contact angle, oil rejection, and PWF. As shown in Fig. 9(a)–(c), the membrane surface contact angle and PWF gradually increased with the increasing of the shaking time; the oil rejection gradually decreased, which may have resulted from the part of hydrophilic PVA leach out from the membrane after shaking. In detail, the contact angle of the fresh CA/PVA membrane (shaking for 0 d) was 63.8˚. After continuously shaking for 9 d, the contact angle increased 6.5% and reached 68.2˚. The PWF increased 28.4%, which might have resulted from the increased membrane porosity caused by the leakage of PVA from the blend membrane partly. As for CA/CPVA membrane, the water contact angle after shaking for 9 d (62.3˚) was slightly higher than that of the fresh membrane (60.4˚). Furthermore, the PWF increased 1.8% only. Compared to the CA/PVA membrane, after partly crosslinking with GA, the chains of CPVA entangled and interacted with CA strongly. Thus, the CPVA would stably entrap in the

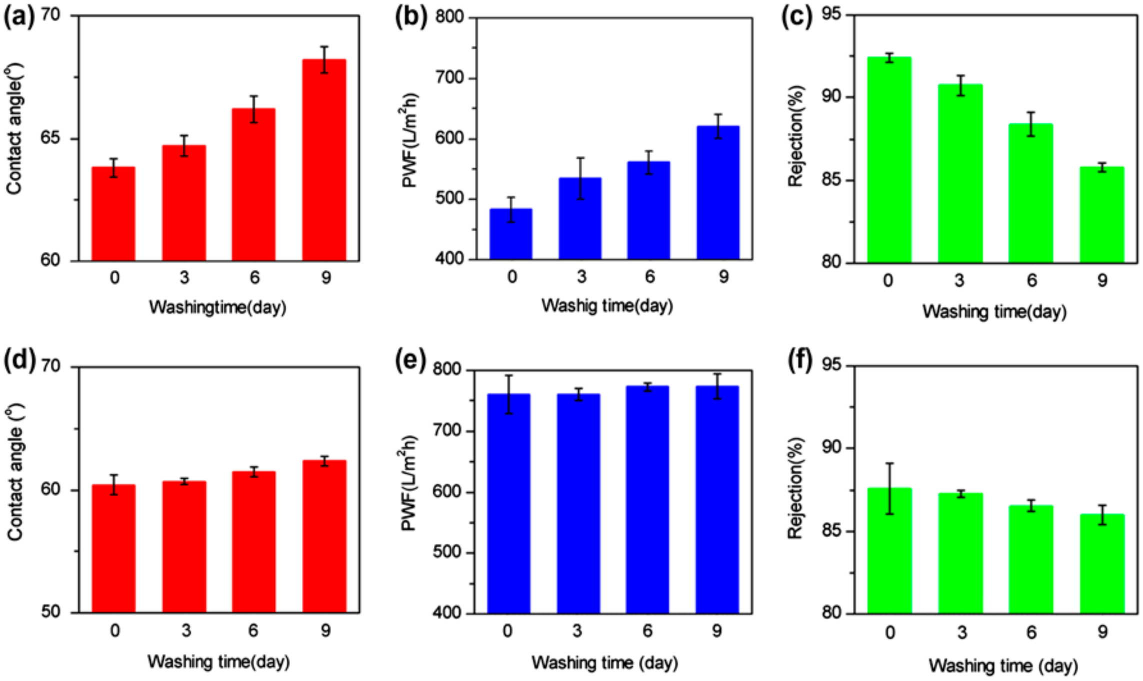

Fig. 9. Water contact angle, PWF and oil rejection of CA/PVA (a, b, and c) and CA/CPVA (d, e, and f) membrane before and after washing. Data were means ± SD (n = 3).

CA membrane and not easily leak out from hybrid membrane in the filtration process.

4. Conclusion

In the present investigation, CA/PVA blend membranes have been first prepared by phase inversion technique without addition of PVP. The PWF, hydrophilicity, and porosity were increased with an increment in CA/PVA compositions up to 90/10. Then, PVP as additive was added into the CA/PVA (90/10) casting solution. The PWF and porosity of CA/PVA/PVP blend membranes increased initially and then declined with the addition of PVP. In the present experiments, the optimal PVP content was 3 wt%, with available PWF (588.1 L/m^2 h) and high oil rejection (91.7%). Meanwhile, the effect of PVP content in the CA/PVA blend membranes on fouling-resistant ability was studied using oil-in-water emulsion. The result indicated that all CA/PVA/PVP blend membranes had better antifouling property than CA/PVA membrane. In order to enhance the stability of the PVA in the blend membrane, PVA was first crosslinked with GA as the crosslinking agent, followed by *in situ* blended with CA and PVP to fabricating the CA/CPVA (80/20)/PVP blend membrane. The optimal content of GA was 0.4 wt% with available PWF (760.2 L/m^2 h) and high FRR (81.2%). After addition of PVP, the CA/CPVA/PVP blend membrane exhibited higher PWF and stronger antifouling ability.

References

[1] D. Sarkar, D. Datta, D. Sen, C. Bhattacharjee, Simulation of continuous stirred rotating disk-membrane module: An approach based on surface renewal theory, Chem. Eng. Sci. 66 (2011) 2554–2567.

[2] H. Wake, Oil refineries: A review of their ecological impacts on the aquatic environment, Estuarine Coastal Shelf Sci. 62 (2005) 131–140.

[3] A. Asatekin, A.M. Mayes, Oil industry wastewater treatment with fouling resistant membranes containing amphiphilic comb copolymers, Environ. Sci. Technol. 43 (2009) 4487–4492.

[4] M. Cheryan, N. Rajagopalan, Membrane processing of oily streams. Wastewater treatment and waste reduction, J. Membr. Sci. 151 (1998) 13–28.

[5] A.A. Al-Shamrani, A. James, H. Xiao, Separation of oil from water by dissolved air flotation, Colloids Surf., A 209 (2002) 15–26.

[6] A. Cambiella, J.M. Bentio, C. Pazos, J. Coca, Centrifugal separation efficiency in the treatment of waste emulsified oils, Chem. Eng. Res. Des. 84 (2006) 69–76.

[7] K.A. Hashmi, H.A. Hamza, J.C. Wilson, CANMET hydrocyclone: An emerging alternative for the treatment of oily waste streams, Miner. Eng. 17 (2004) 643–649.

[8] A. Rezvanpour, R. Roostaazad, M. Hesampour, M. Nystrom, C. Ghotbi, Effective factors in the treatment of kerosene–water emulsion by using UF membranes, J. Hazard. Mater. 16 (2009) 1216–1224.

[9] H.J. Li, Y.M. Cao, J.J. Qin, X.M. Jie, T.H. Wang, J.H. Liu, Q. Yuan, Development and characterization of anti-fouling cellulose hollow fiber UF membranes for oil–water separation, J. Membr. Sci. 279 (2006) 328–335.

[10] W.J. Chen, Y.L. Su, J.M. Peng, X.T. Zhao, Z.Y. Jiang, Y.N. Dong, Y. Zhang, Y.G. Liang, J.Z. Liu, Efficient wastewater treatment by membranes through constructing tunable antifouling membrane surfaces, Environ. Sci. Technol. 45 (2011) 6545–6552.

[11] T. Mohammadi, M. Kazemimoghadam, M. Saadabadi, Modeling of membrane fouling and flux decline in reverse osmosis during separation of oil in water emulsions, Desalination 157 (2003) 369–375.

[12] A. Brehant, V. Bonnelye, M. Perez, Comparison of MF/UF pretreatment with conventional filtration prior to RO membranes for surface seawater desalination, Desalination 144 (2002) 353–360.

[13] S.C.J.M. Van Hoof, J.G. Minnery, B. Mack, Dead-end ultrafiltration as alternative pre-treatment to reverse osmosis in seawater desalination: A case study, Desalination 139 (2001) 161–168.

[14] P.H. Wolf, S. Siverns, S. Monti, UF membranes for RO desalination pretreatment, Desalination 182 (2005) 293–300.

[15] X.L. Ma, Q. Sun, Y.L. Su, Y.Q. Wang, Z.Y. Jiang, Antifouling property improvement of poly(vinyl butyral) ultrafiltration membranes through acid treatment, J. Membr. Sci. 54 (2007) 220–226.

[16] R. Haddad, E. Ferjani, M.S. Roudesli, A. Deratani, Properties of cellulose acetate nanofiltration membranes. Application to brackish water desalination, Desalination 167 (2004) 403–409.

[17] O. Kuttowy, S. Sourirajan, Cellulose acetate ultrafiltration membranes, J. Appl. Polym. Sci. 19 (1975) 1449–1460.

[18] W.J. Chen, Y.L. Su, L.L. Zheng, L.J. Wang, Z.Y. Jiang, The improved oil/water separation performance of cellulose acetate-graft-polyacrylonitrile membranes, J. Membr. Sci. 337 (2009) 98–105.

[19] M. Sivakumar, R. Malaisamy, C.J. Sajitha, D. Mohan, V. Mohan, R. Rangarajan, Ultrafiltration application of CA–PU blend membranes, Eur. Polym. J. 35 (1999) 1647–1651.

[20] C.L. Lv, Y.L. Su, Y.Q. Wang, X.L. Ma, Q. Sun, Z.Y. Jiang, Enhanced permeation performance of cellulose acetate ultrafiltration membrane by incorporation of Pluronic F127, J. Membr. Sci. 294 (2007) 68–74.

[21] R. Mahendran, R. Malaisamy, D. Mohan, Cellulose acetate and polyethersulfone blend ultrafiltration membrane. Part I. Preparation and characterizations, Polym. Adv. Technol. 15 (2004) 149–157.

[22] M. Sivakumar, R. Malaisamy, C.J. Sajitha, D. Mohan, V. Mohan, R. Rangarajan, Preparation and performance of CA–PU blend membrane and their applications-II, J. Membr. Sci. 169 (2000) 215–228.

[23] G. Arthanareeswaran, P. Thanikaivelan, M. Raajenthiren, Fabrication and characterization of CA/PSf/SPEEK ternary blend membranes, Ind. Eng. Chem. Res. 47 (2008) 1488–1494.

[24] R. Malaisamy, R. Mahendran, D. Mohan, M. Rajendran, V. Mohan, Cellulose acetate and sulfonated polysulfone blend ultrafiltration membrane. I. Preparation and characterization, J. Appl. Polym. Sci. 86 (2002) 1749–1761.

[25] S.-G. Kim, K.-H. Lee, Poly(vinyl alcohol) membranes having an integrally skinned asymmetric structure, Mol. Cryst. Liq. Cryst. 512 (2009) 32–39.

[26] Y.Z. Zhang, H.Q. Li, H. Li, R. Li, C.F. Xiao, Preparation and characterization of modified polyvinyl alcohol ultrafiltration membranes, Desalination 192 (2006) 214–223.

[27] S. Zhao, Z. Wang, X. Wei, B.R. Zhao, J.X. Wang, S.B. Yang, S.C. Wang, Performance improvement of polysulfone ultrafiltration membrane using PANiEB as both pore forming agent and hydrophilic modifier, J. Membr. Sci. 385–386 (2011) 251–262.

[28] B. Jung, J.K. Yoon, B. Kim, H.W. Rhee, Effect of molecular weight of polymeric additives on formation, permeation properties and hypochlorite treatment of asymmetric polyacrylonitrile membranes, J. Membr. Sci. 243 (2004) 45–57.

[29] L.Y. Yu, Z.L. Xu, H.M. Shen, H. Yang, Preparation and characterization of PVDF–SiO2 composite hollow fiber UF membrane by sol–gel method, J. Membr. Sci. 337 (2009) 257–265.

[30] A.L. Ahmad, N.M. Yusuf, B.S. Ooi, Preparation and modification of poly(vinyl) alcohol membrane: Effect of crosslinking time towards its morphology, Desalination 287 (2012) 35–40.